

Dramatically Enhanced Efficiency in Ultra-Fast Silicon MSM Photodiodes Via Light Trapping Structures

Hilal Cansizoglu¹, Member, IEEE, Ahmed S. Mayet, Member, IEEE, Soroush Ghandiparsi², Member, IEEE, Yang Gao³, Cesar Bartolo-Perez⁴, Hasina H. Mamtaz, Ekaterina Ponizovskaya Devine, Toshishige Yamada, Senior Member, IEEE, Aly F. Elrefaie, Life Fellow, IEEE, Shih-Yuan Wang, Life Fellow, IEEE, and M. Saif Islam⁵, Senior Member, IEEE

Abstract—Due to relatively low responsivity at near infrared (NIR) wavelengths, surface-illuminated silicon (Si) photodiodes (PDs) are not attractive for ultra-fast data communication applications despite their CMOS-compatibility. Metal-semiconductor-metal (MSM) photodiodes are well-known for simplicity in fabrication compared to pin and pn junctions-based counterparts, but they usually work with lower efficiencies due to thin absorption layer that ensures high speed response. In this letter, we demonstrate a high efficiency and high-speed Si MSM PD with innovative photon-trapping surface structures. These wavelength-scale structures decrease the surface reflection and introduce laterally propagating waves parallel to the semiconductor surface. The responsivity of Si MSM PDs with the photon-trapping holes was measured to be $\sim 0.59\text{A/W}$, while the control devices without holes show $\sim 0.08\text{A/W}$. Such PDs with $50\mu\text{m}$ diameter and with $1\mu\text{m}$ finger spacing provide a pulse response of 60ps and 38ps full-width at half-maximum (FWHM) at 3V and 10V applied bias, respectively. Surface-illuminated PDs with these dimensions can offer easy optical coupling options for fiber optic links while offering complete CMOS compatibility.

Index Terms—Si MSM photodiode, light trapping, broadband absorption, micro-/nanostructures, high-speed, high-efficiency photodetectors.

I. INTRODUCTION

METAL-SEMICONDUCTOR-METAL (MSM) photodiodes (PDs) have long been of interest to the device

Manuscript received May 10, 2019; revised July 31, 2019; accepted August 28, 2019. Date of publication September 5, 2019; date of current version September 20, 2019. This work was supported in part by the Army Research Office (ARO) under Grant W911NF-14-4-0341 and in part by the National Science Foundation (NSF) under Grant CMMI-1235592. (Hilal Cansizoglu and Ahmed S. Mayet contributed equally to this work.) (Corresponding author: M. Saif Islam.)

H. Cansizoglu, A. S. Mayet, S. Ghandiparsi, Y. Gao, C. Bartolo-Perez, H. H. Mamtaz, and M. S. Islam are with the Integrated Nanodevices and Nanosystem Research Group, Department of Electrical and Computer Engineering, University of California at Davis, Davis, CA 95616, USA (e-mail: sislam@ucdavis.edu).

E. Ponizovskaya Devine and S.-Y. Wang are with W&WSens Devices, Inc., Los Altos, CA 94022, USA.

T. Yamada is with the Baskin School of Engineering, University of California at Santa Cruz, Santa Cruz, CA 95064, USA.

A. F. Elrefaie is with the Integrated Nanodevices and Nanosystem Research Group, Department of Electrical and Computer Engineering, University of California at Davis, Davis, CA 95616, USA, and also with W&WSens Devices, Inc., Los Altos, CA 94022, USA.

Color versions of one or more of the figures in this letter are available online at <http://ieeexplore.ieee.org>.

Digital Object Identifier 10.1109/LPT.2019.2939541

engineers for their simple design and FET-compatible fabrication. A commonly adapted device structure has interdigitated metal fingers deposited on a semiconductor to form back-to-back Schottky contacts [1]. MSM PDs have superior speed performance over typical pin or pn diodes by having relatively low capacitance which eliminates RC time limit [2]. Ultra-fast MSM photodiodes have been reported in the literature [3]–[5]. However, they usually suffer from low responsivity, especially at longer wavelengths ($>800\text{ nm}$). This is mainly due to lack of sufficient light penetration into semiconductor since the metal fingers block part of the light. Another reason of low responsivity is weak electric field that occurs deep inside the semiconductor where the photons with longer wavelengths are absorbed and generate photocarriers. However, such carriers can recombine due to insufficient electric field causing lower responsivity. Even if these carriers were collected by such a weak field, they are slow and can degrade the PD performance. Ho et al. proposed to solve this problem with a trench formation in silicon (Si) [6]. Metal contacts at the sidewall of the trenches were formed to create a uniform strong electric field deep underneath the surface. However, increasing the metal contact area can dramatically increase the PD capacitance and cause RC time-limited responses. For that reason, deploying a thin isolated semiconductor layer would be an ideal solution to ensure a uniform strong electric field in an MSM PD. On the other hand, a thin layer of semiconductor would degrade the absorption efficiency of the devices. Si already suffers from low values of absorption coefficient at and just above the indirect bandgap energy (1.12eV). Si absorption is much weaker at a new short wavelength division multiplexing (SWDM) band of 850-950 nm that is being proposed for data center communication [7]. Earlier in the literature, a Si MSM PD with a textured back surface was demonstrated to show 0.17 A/W responsivity at 830 nm while maintaining a -3dB bandwidth of 3 GHz [8]. Several studies show enhancement of light absorption in silicon with surface texturing or structuring at micro/nano scales [9]–[11]

In this letter, we demonstrate a CMOS-compatible surface-illuminated Si MSM PD with a temporal impulse response (a deconvolved response) of 60ps (48ps) and 38ps (27ps) full-width at half-maximum (FWHM) at 3V and 10V applied bias, respectively. Both challenges of increasing the external

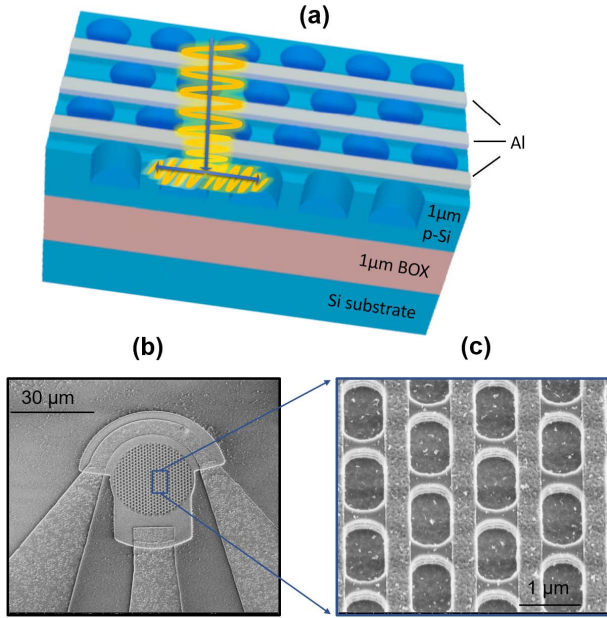


Fig. 1. (a) Illustration of Si MSM PD with holes. Metal fingers are placed in between holes which make light propagate laterally in Si that sits on an SOI substrate with 1 μm BOX (SiO_2) layer, (b) Scanning electron microscopy (SEM) images of a fabricated PD photon-trapping holes. Aluminum (Al) metal fingers are fabricated on Si surface by sputtering and lift-off. A mesa was etched to isolate the devices on SOI substrate and finally a coplanar waveguide (CPW) pattern was fabricated to collect electric signal. (c) A focused SEM image of the PD's active region with photon-trapping holes. Al fingers are seen in between holes. Cylindrical holes have a false-look of elliptical shape because SEM specimen is tilted during imaging.

quantum efficiency (EQE) while maintaining a high-speed operation can be addressed by designing PDs with thin absorption regions integrated with periodic arrays of photon-trapping holes [12]–[16]. Such structures can redirect the Poynting vector of a normal incident optical wave to a laterally propagating light wave parallel to the PD surface. The quantum efficiency of a Si MSM PD with 1 μm thin Si layer on SOI substrate is increased by more than 7 \times (at 3V) and 10 \times (at 10V) compared to a control PD on SOI substrate without photon-trapping holes. This is the first demonstration of a high-speed Si MSM PD integrated with photon-trapping holes providing high quantum efficiency at wavelengths of 800-900 nm.

II. DEVICE SIMULATION, DESIGN AND FABRICATION

Fig. 1(a) shows an illustration of our surface-illuminated innovative Si MSM PD designed with holes, allowing vertically illuminating light laterally propagate inside the Si device layers. Fig. 1 (b) and (c) shows scanning electron microscopy (SEM) images of fabricated devices with holes. CMOS IC compatible processes were employed to facilitate very-large-scale integration (VLSI) and leverage cost reduction.

Si MSM PD was fabricated on a silicon-on-insulator (SOI) substrate that has 1 μm device layer (*p*-Si) with 14-22 ohm.cm resistivity and 1 μm BOX layer. 300 nm wide and 100 nm thick interdigitated aluminum (Al) fingers were fabricated on Si by sputtering and lift-off to form symmetric Schottky contacts. Si surface was cleaned with BOE (6:1) to remove native oxide prior to the metal deposition, which is a key step

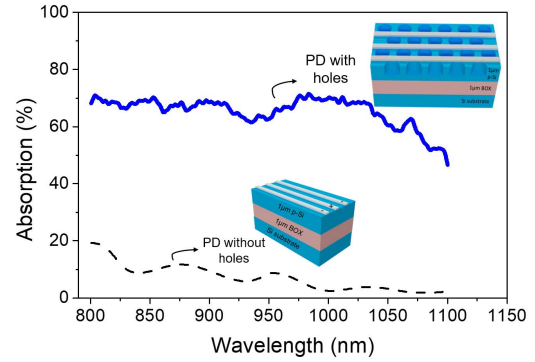


Fig. 2. Absorption vs. wavelength calculated by FDTD method. Both control sample without holes and PD with photon-trapping holes were simulated. The results show distinct difference between optical absorption of the device structure with holes and without holes. Broadband high efficiency with ~ 7 -fold enhancement by photon-trapping holes is predicted by FDTD simulations. On the other hand, light has a two-way path (reflection from bottom Si-SiO₂ interface enables the second path) to get absorbed in Si without holes.

to achieve high speed responses. Afterwards, periodic holes with 1 μm diameter and 1.3 μm period were patterned and etched with a DRIE tool to form 0.6 μm deep cylindrical holes in Si. Subsequently, devices were isolated from each other with a mesa etch and 300 nm Al was deposited, and a lift-off process was applied to create coplanar waveguides (CPW) to transport the electrical pulse converted from a picosecond (ps) light pulse by Si MSM PD. Finally, devices were dipped in hydrofluoric acid ($\text{HF}:\text{H}_2\text{O}$ 1:100) for 3 seconds [17]. A control device without holes was also fabricated in the same process as a comparison.

Fig. 2 shows the results of finite difference time domain (FDTD) simulations calculated by averaging the absorption of light illuminating at various angles ($0^\circ - 10^\circ$). Simulated structure has 1 μm Si on 1 μm SiO₂ layer and 100 nm thick, 300 nm wide Al metal fingers with 1000 nm spacing. Hexagonally packed cylindrical holes with diameter/period (*d/p*) 700/1000 nm are placed in between fingers to increase the light absorption in Si with enhanced lateral light propagation in all directions. In a flat device, photons don't experience perpendicular bending and continue to propagate in the vertical orientation and get reflected back on the bottom Si-SiO₂ interface. This enables a flat PD to exhibit higher absorption compared to flat PDs fabricated on a bulk Si wafer. FDTD simulations predicted that Si MSM PDs with holes can absorb light about $\sim 7\times$ more than PDs without holes for operating wavelengths of 850-950nm. Reduced reflection at air-Si interface and enhanced light penetration and bending in the parallel direction to the surface combined with back reflection from Si-SiO₂ interface result in high optical absorption in Si PDs with integrated holes. Consequently, electron-hole pairs are efficiently generated close to the surface and get drifted under strong lateral electric field in MSM structures. As a result, a high-speed photocurrent can be achieved by an MSM PD that simultaneously exhibits high responsivity. FDTD simulations suggest $\sim 15\%$ reflection loss (not shown here) due to metal fingers in our Si PDs with integrated holes. In future devices, a design with transparent/semi-transparent contacts [18] can reduce the optical loss due to reflected light from metal fingers.

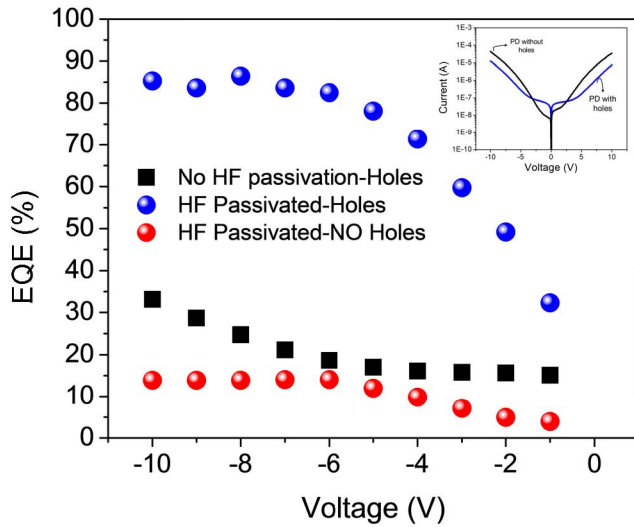


Fig. 3. Measured external quantum efficiency (EQE) of Si MSM PDs with holes and HF passivation (blue), with holes and no HF passivation (black), and no holes with HF passivation (red) at different applied biases. Top-right inset shows logarithmic scale dark current characteristics of Si MSM PDs (with 50 μm device diameter) with and without photon-trapping holes. Black curve indicates PD without holes and blue curve shows dark current of PD with holes.

III. EXPERIMENTAL RESULTS

Fig 3 shows electrical and optical characterization results of Si MSM PDs. The photocurrent is measured with a lock-in amplifier which is fed as a reference signal created by a mechanical chopper at 1 kHz. The impinging light was divided into two fiber patch cords with a splitter and one of them was connected to a fiber probe that delivers the incident light to the device under test while the other one was connected to a power meter to monitor the optical power of incident light in real time. A supercontinuum laser was used to tune the wavelength of the incident light.

The devices with holes that allow lateral propagating waves, experience enhanced photon-matter interactions and result in measured maximum EQE of 86% and 60% at 850 nm when biased with 10V and 3V, respectively (Fig. 3). This proves the efficacy of the photon-trapping holes on enhanced light interaction with the semiconductor. Another advantage of the photon-trapping holes is a broadband high efficiency. Si typically does not respond well to the wavelengths close to the bandgap energy, however, our Si MSM PDs with photon-trapping holes maintain a high efficiency even when they are illuminated with wavelength such as $\lambda = 900$ nm (EQE is measured to be above $> 70\%$ at 10V bias). Such broadband high efficiency and high speed make Si MSM PDs with photon-trapping holes favorable for many important applications.

The inset shows an example of logarithmic IV curve measured from a circular PDs in 50 μm device diameter, with and without photon-trapping holes under dark. Although PDs with holes tend to have higher dark current compared to control sample at relatively low voltages ($< 3\text{V}$), the dark current still stays < 100 nA. At elevated bias ($> 3\text{V}$), dark current increases in both devices, however, dark current in PDs with holes are lower than dark current produced by

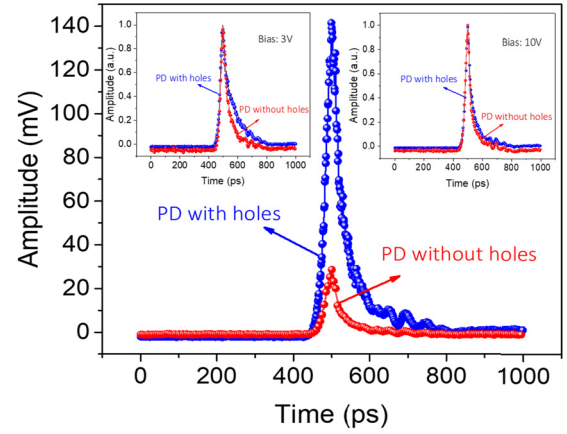


Fig. 4. Measured high speed pulse response at 10V bias from PDs with (blue spheres) and without (red circles) holes. Left and right insets show normalized pulse responses at 10V and 3V applied bias, respectively. The illumination wavelength of pulse light is 850 nm. The FWHM value of the set-up limited temporal response of a PD with and without holes is 38ps and 35ps at 10V applied bias, respectively. The deconvolved response of the device was estimated to be 48ps (3V) and 27ps (10V) at 850 nm.

PDs without holes. An increase in photocurrent with an elevated bias is observed in PDs with holes, indicating a recombination mechanism due to surface states under weak bias. The sidewalls of holes created by DRIE are subject to ion-bombardment during etching process and can be left with dangling bonds that cause surface states. For this reason, dark current and EQE are expected to improve with a more effective surface passivation.

A pulsed laser with ~ 15 ps pulse width and a repetition rate of 70 MHz was used to conduct high-speed measurements on a microwave probe station. A PD with a diameter of 50 μm was tested with a microwave probe and the light beam was aligned with a translational stage to maximize the photocurrent. The electrical pulses were collected by a 20-GHz sampling scope. The PD under test was DC biased using a 25-GHz bias-T.

Fig. 4 shows measured high speed pulse responses of PDs with (blue spheres) and without (red circles) photon-trapping holes at 10V bias. Left and right insets show normalized pulse responses at 10V and 3V applied bias, respectively. The illumination wavelength of pulse light is 850 nm. The FWHM value of the temporal response of a PD with holes was measured as 60ps (at 3V) and 38ps (at 10V). On the other hand, control PD without holes produced a pulse response with 41ps (at 3V) and 35ps (at 10V) FWHM. Si MSM PDs with holes maintain their speed performance while dramatically increasing EQE.

Considering the 22 ps FWHM response for the 20-GHz sampling oscilloscope, and the optical laser pulse width of ~ 15 ps, the actual response of the device was estimated to be 33ps (3V) and 28ps (10V) at 850 nm based on $\tau_{meas} = \sqrt{\tau_{actual}^2 + \tau_{scope}^2 + \tau_{optical}^2}$ where τ_{meas} , τ_{actual} , τ_{scope} and $\tau_{optical}$ are the measured, actual, oscilloscope, and laser optical pulse widths in time domain [19]. This is acceptable for Gaussian pulses and is a valid approximation for our actual measurements.

IV. CONCLUSION

Si-based MSM photodiodes with innovative photon-trapping holes are designed and fabricated with more than 7-fold (at 3V) and 10-fold (at 10V) higher EQE compared to a control PD without holes for wavelengths, $\lambda > 800\text{nm}$. The devices enable the development of efficient high-speed Si PDs suitable for monolithic integration with CMOS electronics for short reach multimode optical data links used in datacom and computer networks. It is anticipated that such improvement in the performance of Si PDs can contribute to cost saving in the transceiver design that are expected to be widely used in the free-space and data communication.

ACKNOWLEDGMENT

The authors would like to thank S.P. Wang and S.Y. Wang Partnership for financial support.

REFERENCES

- [1] S. M. Sze, D. J. Coleman, Jr., and A. Loya, "Current transport in metal-semiconductor-metal (MSM) structures," *Solid-State Electron.*, vol. 14, no. 12, pp. 1209–1218, 1971.
- [2] S. Sze, *Physics of Semiconductor Devices*. Hoboken, NJ, USA: Wiley, 1981.
- [3] B. J. van Zeghbroeck, W. Patrick, J.-M. Halbout, and P. Vettiger, "105-GHz bandwidth metal-semiconductor-metal photodiode," *IEEE Electron Device Lett.*, vol. EDL-9, no. 10, pp. 527–529, Oct. 1988.
- [4] W. Roth, H. Schumacher, J. Kluge, H. Geelen, and H. Beneking, "The DSI diode—A fast large-area optoelectronic detector," *IEEE Trans. Electron Devices*, vol. ED-32, no. 6, pp. 1034–1036, Jun. 1985.
- [5] M. Loken, L. Kappius, S. Manti, and CH. Buchal, "Fabrication of ultrafast Si based MSM photodetector," *Electron. Lett.*, vol. 34, no. 10, pp. 1027–1028, May 1998.
- [6] J. Y. L. Ho and K. S. Wong, "Bandwidth enhancement in silicon metal-semiconductor-metal photodetector by trench formation," *IEEE Photon. Technol. Lett.*, vol. 8, no. 8, pp. 1064–1066, Aug. 1996.
- [7] J. A. Tatum *et al.*, "VCSEL-based interconnects for current and future data centers," *IEEE/OSA J. Lightw. Technol.*, vol. 33, no. 4, pp. 727–732, Feb. 15, 2015.
- [8] H. C. Lee and B. van Zeghbroeck, "A novel high-speed silicon MSM photodetector operating at 830 nm wavelength," *IEEE Electron Device Lett.*, vol. 16, no. 5, pp. 175–177, May 1995.
- [9] J. Lv, T. Zhang, P. Zhang, Y. Zhao, and S. Li, "Review application of nanostructured black silicon," *Nanosc. Res. Lett.*, vol. 13, no. 1, p. 110, 2018.
- [10] P. Zhang, S. Li, C. Liu, X. Wei, Z. Wu, and Y. Jiang, "Near-infrared optical absorption enhanced in black silicon via Ag nanoparticle-induced localized surface plasmon," *Nanosc. Res. Lett.*, vol. 9, no. 1, p. 519, 2014.
- [11] P. Kuang, S. Eyderman, M.-L. Hsieh, A. Post, S. John, and S.-Y. Lin, "Achieving an accurate surface profile of a photonic crystal for near-unity solar absorption in a super thin-film architecture," *ACS Nano*, vol. 10, pp. 6116–6124, Jun. 2016.
- [12] Y. Gao *et al.*, "Photon-trapping microstructures enable high-speed high-efficiency silicon photodiodes," *Nature Photon.*, vol. 11, pp. 301–308, Apr. 2017.
- [13] H. Cansizoglu *et al.*, "Surface-illuminated photon-trapping high-speed Ge-on-Si photodiodes with improved efficiency up to 1700 nm," *Photon. Res.*, vol. 6, no. 7, pp. 734–742, 2018.
- [14] K. Zang *et al.*, "Silicon single-photon avalanche diodes with nanostructured light trapping," *Nature Commun.*, vol. 8, Sep. 2017, Art. no. 628.
- [15] S. Yokogawa *et al.*, "IR sensitivity enhancement of CMOS image sensor with diffractive light trapping pixels," *Sci. Rep.*, vol. 7, Jun. 2017, Art. no. 3832.
- [16] H. Cansizoglu, A. F. Elrefaie, C. Bartolo-Perez, T. Yamada, Y. Gao, and A. S. Mayet, "A new paradigm in high-speed and high-efficiency silicon photodiodes for communication—Part II: Device and VLSI integration challenges for low-dimensional structures," *IEEE Trans. Electron Devices*, vol. 65, no. 2, pp. 382–391, Feb. 2018.
- [17] A. S. Mayet, H. Cansizoglu, Y. Gao, S. Ghandiparsi, A. Kaya, and C. Bartolo-Perez, "Surface passivation of silicon photonic devices with high surface-to-volume-ratio nanostructures," *J. Opt. Soc. Amer. B, Opt. Phys.*, vol. 35, no. 5, pp. 1059–1065, 2018.
- [18] D. G. Parker, P. G. Say, A. M. Hansom, and W. Sibbett, "110 GHz high-efficiency photodiodes fabricated from indium tin oxide/GaAs," *Electron. Lett.*, vol. 23, no. 10, pp. 527–528, May 1987.
- [19] K. Rush, S. Draving, and J. Kerley, "Characterizing high-speed oscilloscopes," *IEEE Spectr.*, vol. 27, no. 9, pp. 38–39, Sep. 1990.